Microelectronic Engineering 86 (2009) 2334–2341

Contents lists available at ScienceDirect

Microelectronic Engineering

journal homepage: www.elsevier.com/locate/mee

An alternative method for fabricating microcontact printing stamps

Gaoshan Jing [a], Joseph P. Labukas [b], Wenyue Zhang [a], Susan F. Perry [d], Shi-Fang Lu [c], Gregory S. Ferguson [b], Svetlana Tatic-Lucic [a,*]

[a] Sherman Fairchild Center, Department of Electrical and Computer Engineering, Lehigh University, 16A Memorial Dr. East, Bethlehem, PA 18015, USA
[b] Department of Chemistry, Lehigh University, USA
[c] Department of Biological Sciences, Lehigh University, USA
[d] Department of Chemical Engineering, Lehigh University, USA

ARTICLE INFO

Article history:
Received 21 November 2008
Accepted 10 April 2009
Available online 19 April 2009

Keywords:
Cell patterning
Microcontact printing
Self-assembled monolayers (SAMs)
Photopatternable silicone

ABSTRACT

In this paper, we describe the development of microcontact printing stamps from photopatternable silicone. The photopatternability of this material enables convenient and fast stamp fabrication, and allows rapid patterning of substrates for culturing biological cells. Microcontact printing stamps made of the photopatternable silicone with linewidths as small as 2 μm were fabricated and reliable cell patterning results were obtained by optimizing the stamping process. An optimal stamp surface was obtained by optimizing the photolithographic process. Our successful demonstration of patterning cells using the photopatternable silicone stamps establishes this alternative approach for fabricating microcontact printing stamps.

1. Introduction

Anchoring cells in predefined patterns on a surface has become very important for the development of cellular biosensor technology, tissue engineering applications, and understanding fundamental cell functions [1–3]. Realization of predefined neural networks *in vitro* is especially important to achieve high-resolution analysis at the electrical, metabolic and structural levels [4,5]. Mammalian neural cells naturally rely on an *in vivo* support network called the **e**xtra**c**ellular **m**atrix (ECM) for survival. Therefore, to pattern these cells in an organized way, their growth can be controlled by patterning the support structure they require. Most tissue engineering applications begin with a specific chemical, controlling where the ECM is affixed, and ultimately where the tissue is able to grow. Alternatively, a chemical which behaves like the ECM can be directly patterned on the substrate, and cell growth can still be controlled.

In order to pattern cells in specific patterns, a common approach is to create cell-attractive regions separated by cell-repulsive regions, so that cells will be bound to the cell-attractive regions without spreading over the adjacent cell-repulsive regions. At present, microcontact printing (μCP) is the most commonly used technique to pattern SAMs or proteins (and thereby cells) on a micrometer scale, and **p**oly**d**i**m**ethyl**s**iloxane (PDMS) is the most frequently used material for microcontact printing [1,6,7].

By printing proteins or self-assembled monolayers (SAMs) on surfaces using PDMS stamps, microcontact printing has become a routine technique for fundamental biological research. For example, PDMS stamps have been used to imprint alkanethiols (forming hydrophobic regions) and thiolated **p**oly**e**thylene **g**lycols (PEGs) (forming protein repulsive regions) on gold, followed by coating with an ECM component (e.g., fibronectin) in the hydrophobic area, which creates non-adhesive regions unsuitable for the cell growth separated by adhesive islands of defined shape and size [8]. Some researchers have also used PDMS stamps to print poly-D-lysine and PEG silane (protein repulsive SAM) directly on a glass surface. Poly-D-lysine is a cell-attractive protein and suitable for the growth of certain cell types, such as hippocampal neurons [9]. There are great advantages for microcontact printing using PDMS stamps, such as low cost and rapid prototyping, however, PDMS stamps have some drawbacks. For instance, PDMS stamps are easily deformed because of their low Young's modulus [10,11].

In this paper, we report the use of a novel material, WL-5351 photopatternable silicone (Dow Corning), to create stamps for microcontact printing. The main motivation for exploring this material is that its photopatternability would enable a simpler fabrication process, without a molding step. Compared with PDMS, this photopatternable silicone has a higher Young's modulus [12]. Its high Young's modulus is expected to reduce the deformability of the stamps. In our previous work, we have formed the photopatternable silicone stamps with a minimum line and spacing resolution of 25 μm [13], which is not fine enough for cell research, where a typical size of mammalian cells suspended in culturing medium is about 10 μm in diameter [14]. We have improved the

* Corresponding author. Tel.: +1 610 758 4552; fax: +1 610 758 6279.
E-mail address: svt2@lehigh.edu (S. Tatic-Lucic).

0167-9317/$ - see front matter © 2009 Elsevier B.V. All rights reserved.
doi:10.1016/j.mee.2009.04.013

resolution of the photopatternable silicone stamps down to 2 μm. We also present here an optimization of the fabrication process for photopatternable silicone stamps based on statistical design of experiments related to the flatness of the contacting surface. Precise cell patterns were thus obtained using stamps made of photopatternable silicone.

2. Materials and methods

The fabrication process for the photopatternable stamps and subsequent patterning of cells on glass slides previously treated by microcontact printing are schematically presented in Fig. 1. First, we fabricated the photopatternable silicone stamps using a photolithographic process. Then, a hydrophobic self-assembled monolayer was printed on a glass substrate using the photopatternable silicone stamp to prevent cell growth. Finally, a hydrophilic SAM suitable for cell growth was coated on the part of the glass surface that was not already hydrophobic, to promote cell growth. Immortalized mouse hypothalamic neurons (GT1-7) were cultured, *in vitro*, on the chip prepared in this fashion. Patterned cells, with or without fluorescent staining, were visualized by an inverted microscope. The details of the individual steps are presented below.

2.1. Photolithographic process for the photopatternable silicone

The photolithographic process for the photopatternable silicone (WL-5351, Dow Corning), which acted as a negative photoresist, was as follows: prior to use, the photopatternable silicone was allowed to equilibrate to room temperature from its storage temperature (−15 °C). The substrate used in this experiment was a 4 inch diameter silicon wafer. First, the silicon wafer was cleaned by a commercial cleaning solution (Nanostrip, Cyantek Inc) for 30 min, then rinsed and dried. Next, the wafer was dehydrated at 150 °C for 30 min in a convection oven. The photopatternable silicone was spin-coated at 500 rpm for 15 s with a ramp rate of 100 rpm/s, and then ramped at 200 rpm/s to a speed of 2500 rpm for 40 s. To reduce edge bead formation, the photopatternable silicone was finally spin-coated at 1500 rpm for 65 s with a decelerating rate of 200 rpm/s. After spin-coating, the film was soft-baked at 110 °C for 4 min on a vacuum hot plate and then exposed to broadband UV with a dose of 1200 mJ/cm^2 using a contact aligner EV620 (EV Group Inc, Albany NY). Following the UV exposure, the film was subjected to a post exposure baking (PEB) at 140 °C for 2.75 min. It is during this step that the UV-irradiated portions of the film undergo a crosslinking process rendering those areas insoluble in the developer [15]. After the photopatternable silicone film was developed in WL-9653 developer (Dow Corning) for 4 min and rinsed in isopropyl alcohol (IPA) for 4 min, the elastomer stamp was hard-baked at 180 °C for 60 min.

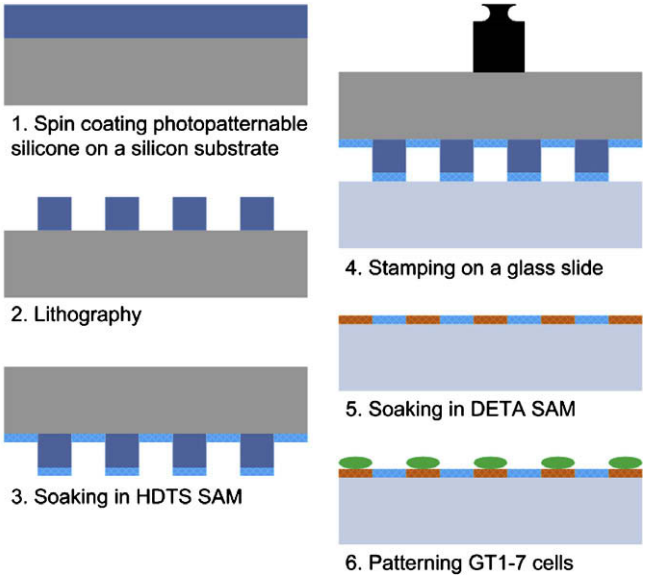

Fig. 1. Schematic of patterning of GT1-7 cells on glass slides by microcontact printing using photopatternable stamps.

2.2. Microcontact printing with photopatternable silicone stamps

The first step after the completion of the stamp fabrication process was to cut photopatternable silicone stamps on a silicon substrate to size (3 cm^2 in area), manually using a diamond scriber. The printing process was as follows: **h**exa**d**ecyl**t**richloro**s**ilane (HDTS), which forms a hydrophobic surface and prevents cells from growing, was inked onto stamps by soaking them in a 7.2 mM solution of HDTS (Gelest Inc., PA) in toluene for 30 s, and then the stamps were blown dry with a stream of nitrogen. The stamps were placed in contact with piranha-cleaned (70% H_2SO_4 and 30% H_2O_2) glass slides. In order to enhance the physical contact of the stamps, a load was applied to this sandwich structure (Fig. 1) for 30 min. For the photopatternable silicone stamps, which have higher Young's modulus than conventionally used polymethyldisiloxane (PDMS) stamps [12], the applied loads tested were 0.67, 1.00, 1.30 and 1.67 MPa. The range of loads was applied in order to determine the minimum load necessary for clear and reproducible patterns. After 30 min, the stamps were carefully removed and the substrate was rinsed with ethanol and deionized water. The substrates were dried with a stream of nitrogen. Finally, a hydrophilic SAM derived from 3-trimethoxysilyl propyl-diethylenetriamine (DETA), a chemical replacement for ECM proteins to facilitate cell adhesion and growth [4], was coated on the regions not already coated with the hydrophobic HDTS SAM by immersing the glass substrate in a 23 mM solution of DETA (Gelest Inc., PA) in methanol for 1 h. The same rinsing and drying steps mentioned above were repeated twice.

2.3. Cell dissociation and culturing

Immortalized mouse hypothalamic neurons (GT1-7) were used to assess the effect of the SAM patterns on the cells' positioning and growth. The GT1-7 cells were maintained in 25 cm^2 flasks (Fisher Scientific, GA) at 37 °C in an incubator with humidified 8% CO_2. The culture medium contained **D**ulbecco's **M**odified **E**agle **M**edium (DMEM) (Gibco, NY), 1 mM sodium pyruvate, 10 mM sodium bicarbonate, 2 mM L-glutamine, 10 mM Hepes buffer and 10% **f**etal **b**ovine **s**erum (FBS, Gibco, NY) [16].

Glass slides patterned with alternating hydrophobic (HDTS) and hydrophilic (DETA) SAM regions were put into six-well cell-culture plates (BD Biosciences, CA). The GT1-7 cells were dissociated by incubating in 0.125% (w/v) trypsin solution at 37 °C for 8 min. Following trypsinization, the cells were pelleted by centrifugation at 750 rpm for 5 min and re-suspended in the culture medium. The cells were plated in the six-well plates at a density of 1×10^5 cells in 5 mL culture medium. The cells were maintained under standard conditions until patterns could be observed (typically 48 h) by optical microscopy.

2.4. Cell imaging by epifluorescent microscopy/phase contrast microscopy

The patterned GT1-7 cells were rinsed with **p**hosphate **b**uffered **s**aline (PBS) solution and placed in serum-free medium (containing

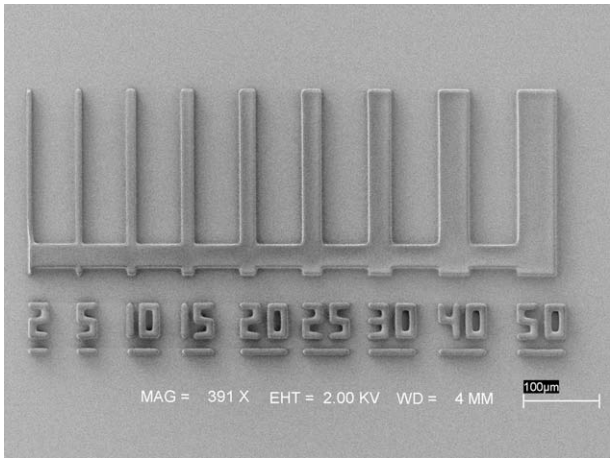

Fig. 2. SEM image of the test structure for photopatternable silicone with an exposure dose 1200 mJ/cm^2, and post exposure baking at 140 °C for 2.75 min. The linewidth varies from 2 to 50 μm separated by 60 μm spacing.

all of the components of the culture medium mentioned above except FBS) in each well. A fluorescent stain, 2 μM calcein AM (Invitrogen Corp., CA), was added to the medium and the cells were incubated at room temperature for 20 min. The stained GT1-7 cells were visualized with an inverted microscope IX70 (Olympus Inc., PA). Phase contrast images were also taken by the same inverted microscope. The scale bars were calibrated with a stage micrometer (OB-M 1/100, Olympus Inc., PA) for different magnifications and added with the SPOT imaging software (Diagnostic Instruments, MI).

3. Results and discussion

In our experiments, we have focused on three areas: (1) determining the best photolithographic resolution that can be achieved using photopatternable silicone; (2) optimizing the photolithographic process to obtain the optimal stamping surface; (3) optimizing the stamping process to get reliable patterning results.

First, we explored the photolithographic resolution of the photopatternable silicone. The typical thickness range for the

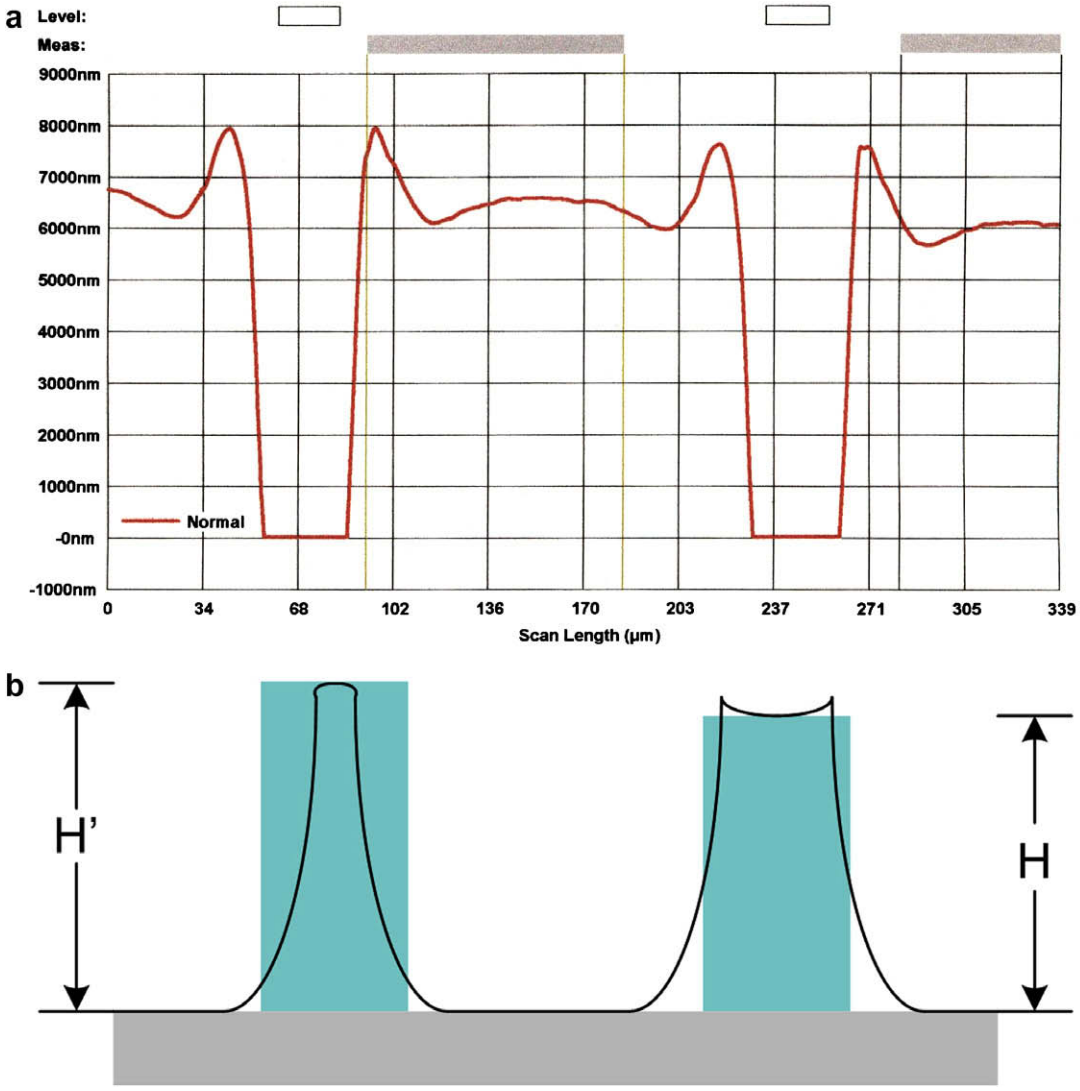

Fig. 3. (a) Profilometer measurements of the surface topology of photopatternable silicone stamps. Note the bumps at the edges of the lines. (b) The measurement scheme for different shapes of lines. If there were no bumps on a line, we measured the full height of the line; if there were bumps on a line, we measured the distance between the substrate and the line's region between the bumps as the height of the line.

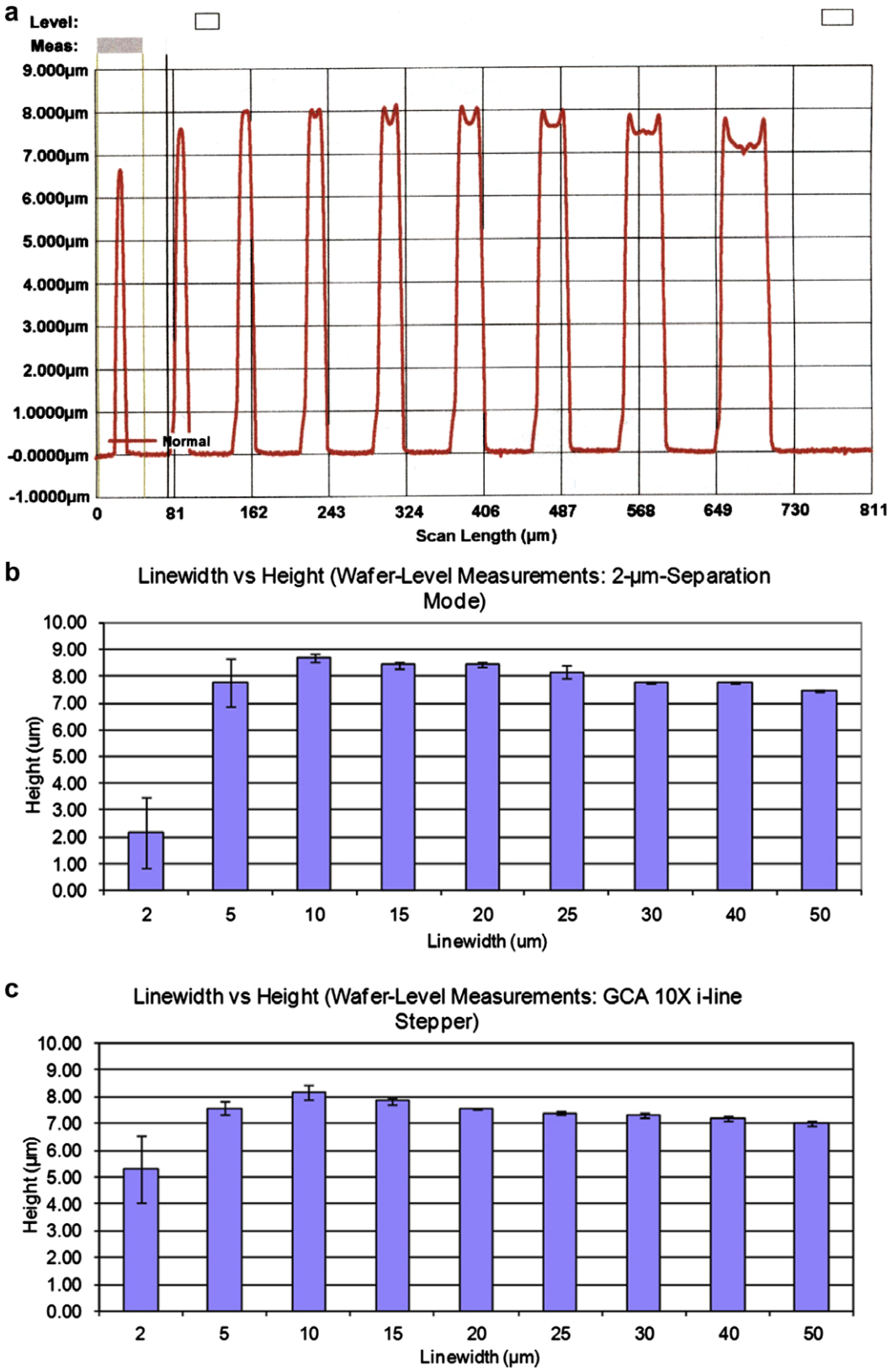

Fig. 4. (a) Profilometer measurements of the surface topology of the photopatternable silicone test structure with linewidths varying from 2 to 50 µm. The spacing between the lines was 60 µm. (b) The relationship between feature height and linewidth of the photopatternable silicone stamps fabricated using a contact aligner EV620 and proximity contact mode with a 2 µm separation. The measurements were performed on five dies uniformly distributed over a 4 inch wafer. (c) The relationship between feature height and linewidth of the photopatternable stamps fabricated using a GCA 10X i-line stepper. The measurements were performed on five dies uniformly distributed over a 4 inch wafer.

photopatternable silicone is 6 to 18 μm and the recommended spin speed is 500 to 2500 rpm [15]. Here we use 2500 rpm to obtain thinner films so that we could achieve the best resolution within manufacturer recommended thicknesses for this material during photolithographic steps. The best resolution we were able to achieve is 2 micron (exposure dose 1200 mJ/cm^2 using contact aligner, post exposure baking temperature at 140 °C for 2.75 min), as shown in Fig. 2. Higher exposure doses such as 1400 mJ/cm^2, which were implemented to optimize the profile of the exposed lines (as explained in later portions of this section), have resulted in slightly overexposed features, by lowering the resolution to approximately 5 microns, which is sufficiently fine for patterning mammalian cells.

The issue that we had observed during our initial experiments was the unusual shape of the lines formed in photopatternable silicone upon the completion of photolithographic process (including the exposure, development and post baking process). Specifically, we have observed a slope of the profile with slight bumps at the edge of the flat patterned lines, as illustrated in Fig. 3a. Experimental results from other research groups also show the existence of the bumps [17,18]. The underlying reason is still not clear and it is under investigation.

We have investigated the prominence of these bumps as a function of the linewidth. First, it was necessary to clarify the way of measuring the bump height. Our measurement scheme is illustrated in Fig. 3b and was as follows: if there were no bumps on a line (which was the case with very thin lines), we measured the full height of the line; if there were bumps at the edges of a line, we measured the distance between the substrate and the line's region between the bumps as the height of the line.

By measuring the heights of structures with a P10 profilometer (KLA-Tencor, San Jose, CA) as shown in Fig. 4a, we found that lines with different widths had different heights. For features produced with a 2 μm separation proximity contact mode, as shown in Fig. 4b, five measurements were performed for lines with different widths on five dies uniformly distributed over a 4 inch wafer. The 2 μm lines had the smallest average height (2.81 μm), and 10 μm lines had the biggest average height (8.82 μm). As the linewidth was gradually increased to 50 μm, the height dropped to 7.31 μm; eventually, the film thickness tapered down to 6.66 μm for lines with a width of 1 mm.

Alternatively, we also used a GCA 10X i-line stepper to perform the exposure, and the optimum exposure dose for this purpose was found to be 1800 mJ/cm^2. A similar trend for height of lines of the photopatternable polymer was found as for line heights obtained using contact aligner exposure, as illustrated in Fig. 4c, in which five different measurements were performed for each linewidth on five dies uniformly distributed over a 4 inch wafer. The average height was smallest, 5.09 μm, for 2 μm wide lines and biggest (8.17 μm) for 10 μm wide lines. The average height dropped to 7.01 μm when the linewidth was gradually increased to 50 μm; eventually, the film thickness decreased to 6.47 μm for lines with a width of 1 mm. Using a stepper did not improve the photopatternable silicone patterns, nor could bumps at the edge of lines be eliminated, so the projection mode was not better than the 2 μm separation proximity contact mode we used for processing the photopatternable silicone.

In the following section, we will describe our optimization process for the bump minimization. In order to minimize the bump height at the edges of WL-5351 lines to get higher cell patterning resolution, we used method of design of experiments (DOE) to optimize the processing conditions. Then, we used MiniTAB software to analyze our experimental results. We identified three parameters which have the most influence on the bump height: A: exposure dose, B: **p**ost exposure **b**aking (PEB) temperature, and C: PEB time. Then, we determined the boundary values for each parameter in this designed experiment: the exposure dose was between 1000 and 1400 mJ/cm^2, the PEB temperature was between 130 and 150 °C, and the PEB time was between 2 and 3.5 min. The reasons for the choice of boundary condition values, above, are: (1) when the exposure dose was below 1000 mJ/cm^2 or above 1400 mJ/cm^2, the desirable low resolution (2 microns) for the photopatternable silicone was not obtained; and (2) when the PEB temperature was higher than 160 °C and PEB time was longer than 4 min, an undeveloped residue of the photopatternable silicone resurfaced on the surface. The total number of experiments analyzed was eighteen, including executing each possible parameter combination twice. We also included the experimental center point, in order to estimate the curvature of the experiment, and that was repeated twice as well. The design table with experimental bump heights is shown in Table 1.

Using the MiniTAB software, (see Pareto chart shown in Fig. 5a), we found that the main factors affecting the bump height are PEB temperature and PEB time. From the main effects plot generated by MiniTAB shown in Fig. 5b, we determined that higher PEB temperature and longer PEB time lead to a smaller bump height of WL-5351. In contrast, the exposure dose affects the resolution of this photopatternable silicon, but it has little effect on bump

Table 1
Design of experiment (DOE) table for optimizing the photolithographic processing of the photopatternable silicone using a contact aligner EV620 and proximity contact mode with a 2 μm separation.

Run order	Exposure dose (mJ/cm^2)	PEB temperature (°C)	PEB Time (min)	Bump (μm)
1	1400	130	2	2.90
2	1400	130	3.5	1.80
3	1400	150	2	1.51
4	1400	130	2	2.91
5	1400	150	2	1.63
6	1000	150	2	1.53
7	1000	150	2	1.54
8	1000	130	3.5	2.14
9	1000	130	2	2.36
10	1000	150	3.5	0.77
11	1200	140	2.75	2.18
12	1000	150	3.5	1.1
13	1400	150	3.5	1.49
14	1000	130	2	2.91
15	1000	130	3.5	2.11
16	1400	130	3.5	1.91
17	1400	150	3.5	0.84
18	1200	140	2.75	1.54

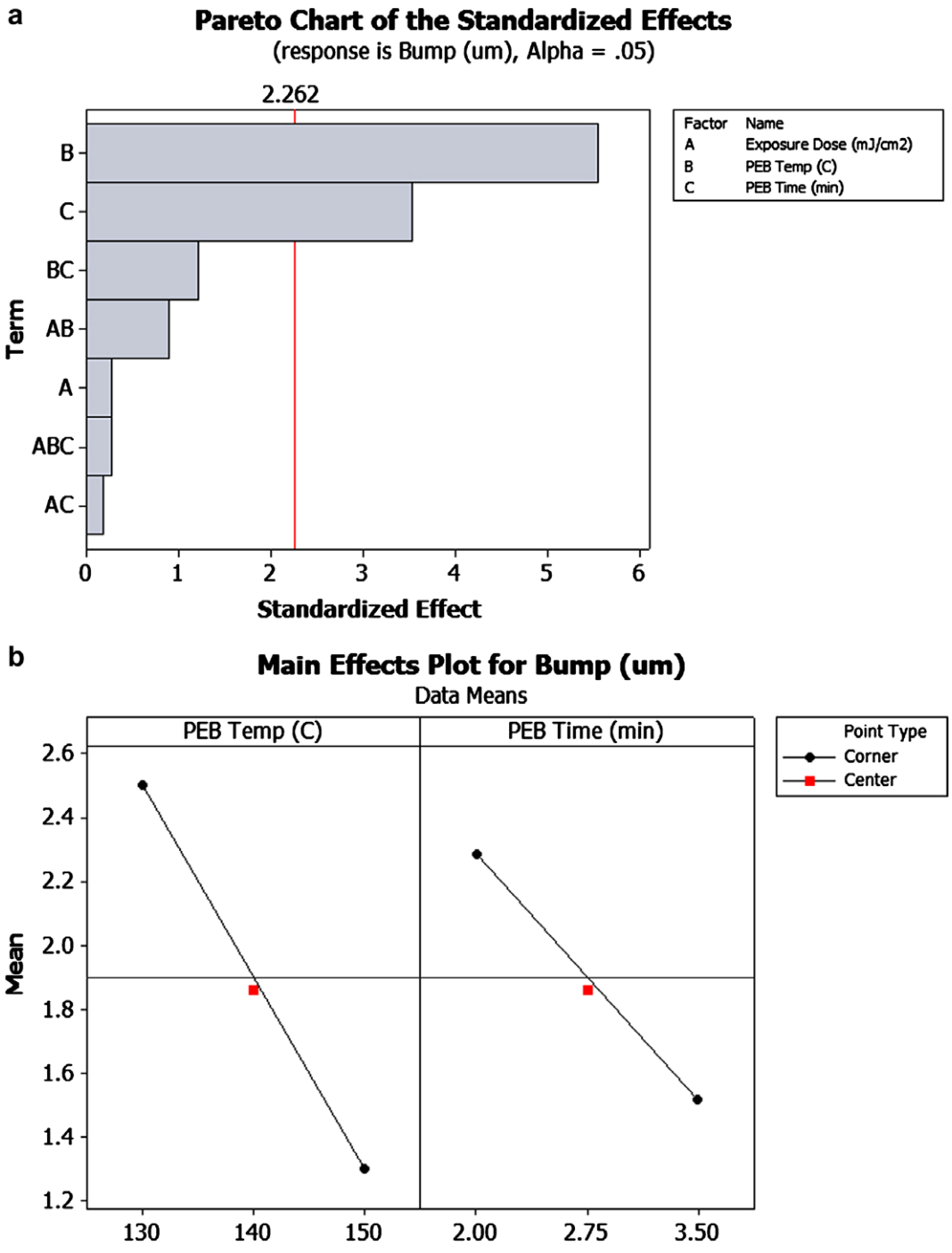

Fig. 5. (a) Pareto chart of the standardized effects of different parameters on bump heights of the photopatternable silicone. The vertical line indicated the value of the minimum significant factor, which was 2.262. (b) The main effects of the standardized effects of different parameters on bump height of WL-5351. The circular dots were boundary conditions for **p**ost **e**xposure **b**aking (PEB) temperature and PEB time. The square dots were center points for the PEB temperature and PEB time.

height. The curvature calculated from this set of experimental data, 0.019, is much smaller than the minimum significant curvature, which is 0.53. So we conclude that the relationship between bump height and PEB temperature is linear between the boundary values, as is the relationship between bump height and PEB time. However, we cannot increase the PEB temperature and PEB time without limit because there will be undeveloped residue of the photopatternable silicone on the surface if the PEB temperature is higher than 160 °C and PEB time is longer than 4 min. We find the average bump height, which is 0.94 μm, is the smallest under the exposure dose of 1000 mJ/cm^2, post exposure temperature of 150 °C, and post exposure baking time of 3.5 min. The optimal recipe for the bump height minimization is as follows: exposure dose of 1000 mJ/cm^2; post exposure baking temperature of 150 °C; post exposure baking time of 3.5 min.

One more fabrication detail should be highlighted here: the surface of the photopatternable silicone was still sticky after soft-baking, so hard contact between the aligner and the photopatternable films is not recommended. In order to get better resolution when using the EV620 contact aligner to expose photopatternable

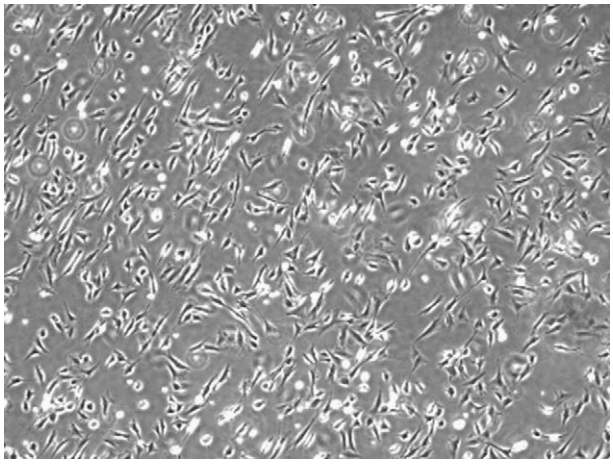

Fig. 6. GT1-7 cells overgrew to hydrophobic regions after 2 days of cell growth patterned using a photopatternable silicone stamp and the load of 1.67 MPa under phase contrast mode. The stamping time was 5 min.

polymer, we recommend using proximity contact with a 2 μm separation between the mask and the photoresist-covered surface of the wafer.

Another parameter that needed optimization was the duration of the stamping process, which defined our hydrophobic areas. We have discovered that an insufficient stamping time results in incomplete SAM coverage (shown in Fig. 6) and subsequently, in an overgrowth of the cells on this patterned substrate. Namely, the cells we cultured here, immortalized mouse hypothalamic neurons (GT1-7), tended to overgrow the incomplete hydrophobic areas, and the intended pattern was no longer visible. Therefore, to get a uniform HDTS SAM films, we performed stamping for 30 min using our photopatternable silicone stamps. When this stamping duration time was used, GT1-7 neuronal cells did not populate the hydrophobic surfaces, defined by the SAM derived from HDTS. Instead, they grew on the hydrophilic surface derived from DETA, (see Fig. 7b and c) and accurately matched the corresponding photopatternable silicone stamp patterns shown in Fig. 7a.

In this work, we achieved higher resolution for WL-5351 patterns and minimized the bumps on the edge of the lines. However, we could not completely eliminate bumps on photopatternable silicone lines wider than ten microns. Bumps at the edge of the lines, as well as the relatively high Young's modulus of the photopatternable silicone, made larger loads necessary for good contact. When the applied load is lower than 1 MPa, GT1-7 cells will overgrow the hydrophobic region and the desired pattern is not visible. Our conclusion is that the hydrophobic SAM was not transferred completely using this pressure. We have found that a load of 1 MPa is the minimum load that yields clear and repeatable cell patterns. Loads higher than 1 MPa do not increase the cell patterning resolution in our experiment and increase the likelihood of die fracture. Roof collapse deformation of the silicone stamp has never been observed when using our optimal pressure whereas it was observed for PDMS stamps for the pressure of 83 kPa.

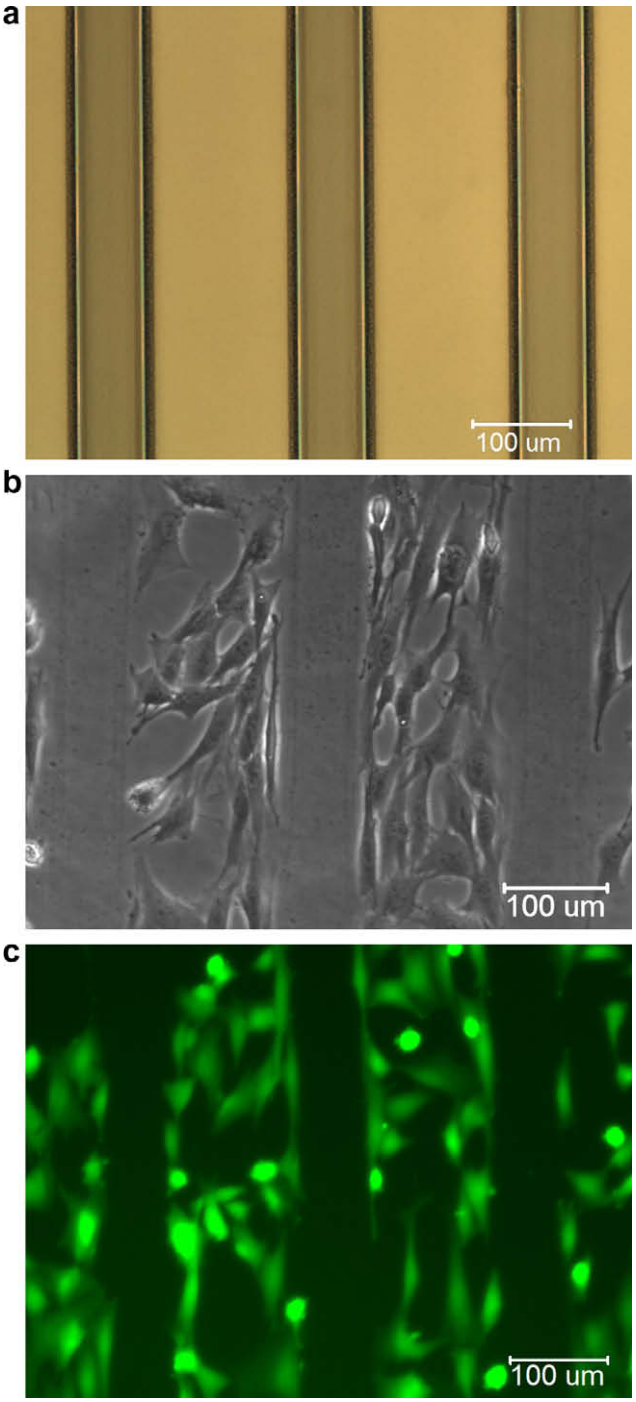

Fig. 7. (a) The photopatternable silicone stamp had 50 μm wide ridges inked with HDTS (hydrophobic). (b) GT1-7 cells after two days of cell growth patterned using a photopatternable silicone stamp under phase contrast mode. (c) Fluorescently stained GT1-7 cells after 2 days of cell growth patterned using a photopatternable silicone stamp and a 1 MPa load.

4. Conclusion

A convenient, alternative microfabrication method to generate stamps for microcontact printing was developed. Microcontact printing stamps were fabricated from a photopatternable silicone, with a linewidth as small as 2 μm. We determined that a 30 min stamping time was required to obtain reliable cell patterning. It was observed that there is a slope of the profile, with slight bumps at the edge of the flat patterned lines. We also established that exposure dose and exposure mode (contact mode or projection mode) did not affect the bump heights at the edge of lines while they did affect the resolution of the photopatternable silicone. Although we were not able to completely eliminate bumps, by increasing the post exposure temperature and post exposure baking time, we could minimize the bumps at the edge of line.

Due to the existence of these bumps at the edge of the flat patterned lines, the obtained cell patterning resolution was larger than the photolithographic resolution of the photopatternable silicone stamps. It was determined that 1 MPa was the minimum load that yields clear and repeatable cell patterns. Sharp and precise hydrophobic patterns were made by contact printing using stamps made of photopatternable silicone and the corresponding cell growth pattern was observed and repeatedly obtained.

Acknowledgements

This work was supported by National Science Foundation (NSF) Career Grant ECS-0448886 and Pennsylvania Infrastructure Technology Alliance (PITA) Grant PA-DCED C000016682. The microfabrication part of this work was performed at the Cornell NanoScale Facility (CNF), a member of the National Nanotechnology Infrastructure Network which is supported by the National Science Foundation (Grant ECS 03-35765), and at the Sherman Fairchild Center at Lehigh University. The WL-5351 photopatternable silicone was provided by Dow Corning Corp.

References

[1] Y. Xia, G.M. Whitesides, Angewandte Chemie International Edition 37 (1998) 550.
[2] C.D.W. Wilkinson, A.S.G. Curtis, J. Crossan, Journal of Vacuum Science & Technology B: Microelectronics and Nanometer Structures 16 (1998) 3132.
[3] W.F. Liu, C.S. Chen, Materials Today 12 (2005) 28.
[4] J.J. Hickman, D.A. Stenger, Enabling Technologies for Cultured Neural Networks, Academic Press Inc., San Diego, 1994. p. 51.
[5] B.C. Wheeler, J.M. Corey, G.J. Brewer, D.W. Branch, Journal of Biomechanical Engineering 121 (1999) 73.
[6] R.S. Kane, S. Takayama, E. Ostuni, D.E. Ingber, G.M. Whitesides, Biomaterials 20 (1999) 2363.
[7] M. Textor, D. Falconnet, G. Csucs, H.M. Grandin, Biomaterials 27 (2006) 3044.
[8] L.E. Dike, S. Chen, M. Mrksich, J. Tien, G.M. Whitesides, D.E. Ingber, In Vitro Cellular & Developmental Biology – Animal 35 (1999) 441.
[9] D.W. Branch, B.C. Wheeler, G.J. Brewer, D.E. Leckband, IEEE Transactions on Biomedical Engineering 47 (2000) 290.
[10] C.Y. Hui, A. Jagota, Y.Y. Lin, E.J. Kramer, Langmuir 18 (2002) 1394.
[11] K.G. Sharp, G.S. Blackman, N.J. Glassmaker, A. Jagota, C.-Y. Hui, Langmuir 20 (2004) 6430.
[12] W. Zhang, J.P. Labukas, S. Tatic-Lucic, L. Larson, T. Bannuru, R.P. Vinci, G.S. Ferguson, Sensors and Actuators A: Physical (2005) 123C–124C.
[13] S. Tatic-Lucic, G. Jing, J.P. Labukas, W. Zhang, S.-F. Lu, S.F. Perry, G.S. Ferguson, in: Eurosensor XX, Göteborg, Sweden, 2006, p. 192.
[14] B. Alberts, A. Johnson, J. Lewis, M. Raff, K. Roberts, P. Walter, Molecular Biology of the Cell, fourth ed., Garland, New York, 2002.
[15] B.R. Harkness, G.B. Gardner, J.S. Alger, M.R. Cummings, J. Princing, Y. Lee, H. Meynen, M. Gonzales, B. Vandevelde, M.V. Bulcke, Proceedings of SPIE 5376 (2004) 517.
[16] Z. Liposits, I. Merchenthaler, W.C. Wetsel, J.J. Reid, P.L. Mellon, R.I. Weiner, A. Negro-Vilar, Endocrinology 129 (1991) 1575.
[17] H. Meynen, M. Vanden Bulcke, M. Gonzalez, B. Harkness, G. Gardner, J. Sudbury-Holtschlag, B. Vandevelde, C. Winters, E. Beyne, Microelectronic Engineering 76 (2004) 212.
[18] S.P. Desai, B.M. Taff, J. Voldman, Langmuir 28 (2007) 575.